Single-End Polarization Mode Dispersion Measurement Using Backreflected Spectra Through a Linear Polarizer

Andrea Galtarossa, *Member, IEEE,* Luca Palmieri, *Member, IEEE,* Marco Schiano, *Member, IEEE,* and Tiziana Tambosso, *Member, IEEE*

***Abstract*—Routine characterization of polarization mode dispersion of single-mode fibers in installed cables requires simple and fast techniques. All standardized techniques use both fiber ends, one connected to the optical source and the other one for signal detection. Clearly, this causes several drawbacks in field tests because the two fiber ends are usually far from each other. Among standardized techniques, the fixed-polarizer method (also called wavelength-scanning method) is one of the simplest to implement. In this work we present a new single-end measurement scheme based on the fixed polarizer method applied to the signal backreflected by the fiber far-end. We report analytical equations and numerical solutions that permit to calculate the mean value of the differential group delay measuring the crossings and/or extrema densities of the spectrum transmitted through a linear polarizer. We also show that the mean value of the differential group delay can be calculated using the Fourier transform of the detected signal. Finally, experimental results on cascades of single-mode step-index fibers confirm the robustness and easiness of our proposal for polarization mode dispersion measurements.**

***Index Terms*—Differential group delay, polarization mode dispersion (PMD).**

I. Introduction

IT is widely accepted that polarization mode dispersion (PMD) is the ultimate limit for optical system performances. Furthermore, its random nature does not allow an easy compensation, as happens for chromatic dispersion which is a deterministic effect. Clearly, measurements are very useful not only before and after cable manufacturing, but also on installed and in-service systems, because PMD evolves as a function of time, depending on environmental changes. Several PMD measurement techniques have been standardized: Jones matrix eigenanalysis (JME) method, fixed-polarizer (FP) method, Poincaré sphere (PS) method and interferometric method. The main drawback of all these methods is that they have to use both fiber ends, one for transmission and the other one for detection. Such a solution is very simple to apply in factory, while it may be more difficult in field tests.

Recently, we suggested to perform PMD measurements by means of the analysis of the state of polarization (SOP) of the backscattered signal. This can be done using a continuous-wave as well as a pulsed source. In [1], a polarization optical time-domain reflectometer (POTDR) scheme was proposed based on a pulsed, temperature-tuned, DFB laser diode. The differential group delay (DGD) was measured by applying the PS method to the Rayleigh backscattered field. The same scheme was also used to measure the mean value of the beat-length [1], [2]. On the contrary, in [3] a different technique was proposed where the optical source was a continuous-wave, external cavity laser diode, and the PMD was characterized by analyzing the SOP of the signal due to the Fresnel far-end reflection.

Both solutions permit to measure the DGD using only one-fiber end, although only the POTDR could measure the mean beat-length and the local evolution of the DGD. However, nowadays POTDR equipments are uneasy to use in field tests. On the contrary, the continuous-wave scheme is based on already available commercial instruments, and it requires a very simple setup.

The purpose of this paper is to describe a new measurement technique based on the continuous-wave (CW) scheme. In particular, we establish accurate relationships between the mean value of the DGD and the extrema density and the level-crossing density of the backreflected signal passing through a linear polarizer. We also show that the same DGD can be calculated analyzing the spectral density of the signal; we name this solution the pseudointerferometric (PI) method.

The extension of the FP and PI methods to the backreflected signal is not trivial, because the statistical distribution of the SOP and of the dispersion vector for fibers in the so-called "long length regime" are very different in forward propagation with respect to the round-trip configuration, as shown in [1], [4]. As a basic example, the DGD of the round-trip follows a Rayleigh distribution while the DGD in forward direction follows a Maxwell distribution.

In this paper we also find analytically the probability density function (pdf) of the three components of the polarization dispersion vector of the round-trip. Moreover, we numerically investigate the influence of the frequency window on measurement accuracy. Finally, several experimental results are presented that show a very good agreement with analytical and numerical predictions.

II. Theoretical Background

The measurement techniques we are going to describe are based on the analysis of the backreflected field. The

Manuscript received February 24, 1999; revised June 6, 1999.

A. Galtarossa and L. Palmieri are with the Dipartimento di Elettronica ed Informatica (DEI), Università di Padova, Padova 35131 Italy.

M. Schiano and T. Tambosso are with the Centro Studi e Laboratori Telecomunicazioni (CSELT), Torino 10148 Italy.

Publisher Item Identifier S 0733-8724(99)08002-0.

total backscattered power is given by two contributions: the Rayleigh scattering (RS), that is a distributed effect, and the Fresnel reflection (FR) from the fiber far-end. Both these contributions may be used to analyze the PMD properties of a fiber. Moreover, Rayleigh backscattering as well as Fresnel reflection are usually modeled as ideal reflectors [5], so that from a theoretical point of view they can be described by the same model. The main difference is in the experimental set-up. In fact, if you are interested in RS, you have to use a pulsed-source in transmission and a time-resolved polarimeter in detection. On the contrary, if you can assume that FR is dominant with respect to RS, then it will be sufficient to use a continuous-wave optical source in transmission and a standard polarimeter in detection. It may be easily verified [6], that if the fiber far-end is well cleaved, and the fiber length is in the order of 50 km or less, then FR is indeed the dominant component of the backscattered power and RS can be neglected (as we will do in the remainder of this paper). This is still more true if one considers that the RS of the whole fiber is almost unpolarized, while the FR is not.

The evolution of the SOP of the far end backreflected field can be conveniently described by means of Stokes vectors and Müller formalism. In fact, let $\hat{s}_F(\omega)$ be the unit Stokes vector at the output of a loss-less, single-mode fiber. Then $\hat{s}_F(\omega) = \mathbf{R}(\omega)\hat{s}_0$, where $\mathbf{R}(\omega)$ is the Müller matrix of the fiber, and $\hat{s}_0$ is the input SOP. The frequency dependence of $\hat{s}_F$ can be explicitly written by means of the following differential equation [7]:

$$\hat{s}'_F = \mathbf{R}'\mathbf{R}^{-1}\hat{s}_F = \bar{\Omega} \times \hat{s}_F \tag{1}$$

where the primes indicate the derivative with respect to ω, and $\mathbf{R}^{-1}$ is the inverse matrix of $\mathbf{R}$. The vector $\bar{\Omega} = (\Omega_1, \Omega_2, \Omega_3)$ is the well-known polarization dispersion vector, and its modulus is equal to the DGD, $\Delta\tau$.

Analogous results had been obtained for backreflected field, i.e., the field that forward propagates up to the fiber far end, undergoes Fresnel reflection, and then back propagates down to the fiber near end. Let $\hat{s}_B(\omega)$ be the Stokes unit vector of such field, it reads [1], [3]

$$\hat{s}_B(\omega) = \mathbf{R}_B(\omega)\hat{s}_0 = \mathbf{M}\mathbf{R}^T(\omega)\mathbf{M}\mathbf{R}(\omega)\hat{s}_0 \tag{2}$$

where $\mathbf{R}_B$ is the Müller matrix representing the round-trip propagation, $\mathbf{R}^T$ is the transpose of $\mathbf{R}$ and $\mathbf{M} = \mathrm{diag}(1, 1, -1)$. Similarly to (1), the dependence of $\hat{s}_B$ on frequency can be expressed as

$$\hat{s}'_B = \mathbf{R}'_B\mathbf{R}_B^{-1}\hat{s}_F = \bar{\Omega}_B \times \hat{s}_B \tag{3}$$

where $\bar{\Omega}_B$ is given by [1], [3]

$$\bar{\Omega}_B = \begin{pmatrix} \Omega_{B1} \\ \Omega_{B2} \\ \Omega_{B3} \end{pmatrix} = 2\mathbf{M}\mathbf{R}^T \begin{pmatrix} \Omega_1 \\ \Omega_2 \\ 0 \end{pmatrix} = 2\mathbf{M}\mathbf{R}^T\bar{\Omega}_L \tag{4}$$

and its modulus is equal to the round-trip DGD, which results $\Delta\tau_B = 2\sqrt{\Omega_1^2 + \Omega_2^2}$.

In this paper we will always deal with fibers in the *long length regime*. Because of this, all the quantities introduced up to now have to be described in terms of their statistical properties. In particular, it is known that $\hat{s}_F$ covers uniformly the Poincarè sphere, independently of the input SOP [8]. Hence, if we rewrite $\hat{s}_F$ in function of its angular coordinates ξ and ψ,

$$\hat{s}_F = (\cos\xi\cos\psi, \cos\xi\sin\psi, \sin\xi) \tag{5}$$

then ξ and ψ are statistically independent random variables with the pdf derived in Appendix A.

The randomness of $\hat{s}_F$ is a consequence of the randomness of $\bar{\Omega}$. It is well known that Ω_i $(i = 1, 2, 3)$ are Gaussian random variables, statistically independent of each other, with zero mean and the same standard deviation. Therefore, $\Delta\tau$ is Maxwell distributed, while $\Delta\tau_B$ is Rayleigh distributed, and the following relationship holds between their mean values [1]:

$$\langle\Delta\tau_B\rangle = \frac{\pi}{2}\langle\Delta\tau\rangle. \tag{6}$$

A. Statistical Description of $\bar{\Omega}_B$

Let us introduce the analytical description of the statistical distribution of $\bar{\Omega}_B$. In [3] it was shown that the pdf of Ω_{Bi} $(i = 1, 2, 3)$ obtained by numerical simulations agreed very well with the experimental one. Moreover, it was also shown that both of them were close to a soliton shaped pdf.

In order to find the analytical expression of the statistical description of Ω_{Bi}, let us show that when the fiber is in the long-length regime each column of the matrix $\mathbf{R}$ is an unit vector that uniformly covers a sphere with unit radius. In fact, if we set $\hat{s}_0 = (1, 0, 0)$, then $\hat{s}_F = \mathbf{R}\hat{s}_0$ is the first column of $\mathbf{R}$. Similarly to (5) let us write this column as

$$\hat{c} = (\cos\mu\cos\eta, \cos\mu\sin\eta, \sin\mu). \tag{7}$$

It is also useful to write $\bar{\Omega}_L$ as follows:

$$\bar{\Omega}_L = \frac{\Delta\tau_B}{2}(\cos\theta, \sin\theta, 0) \tag{8}$$

where θ results to be flat distributed between 0 and 2π (i.e. $\theta \in \mathcal{U}(0, 2\pi)$) and statistically independent of $\Delta\tau_B$ (these are all consequences of the statistical properties of Ω_1 and Ω_2. See for example [9]).

By means of (4) and (7), we can calculate the first component of $\bar{\Omega}_B$, which yields

$$\Omega_{B1} = 2\hat{c}\cdot\bar{\Omega}_L = \Delta\tau_B\cos\mu\cos(\eta - \theta). \tag{9}$$

It is reasonable to assume the elements of $\bar{\Omega}_L$ to be statistically independent of those of $\mathbf{R}$; the rightness of this assumption will be confirmed by experimental and numerical results. From Appendix C we can say that $\cos(\eta - \theta)$ has the same statistical properties of $\cos\eta$, and hence $q = \cos\mu\cos(\eta - \theta)$ is flat distributed between -1 and 1, like the first component of vector $\hat{s}_F$. Finally, recalling that $\Delta\tau_B$ is Rayleigh distributed and statistically independent of q, by means of (B6) we can state that the pdf of Ω_{B1} reads

$$f_{\Omega_{B1}}(a) = \frac{\pi}{4\langle\Delta\tau_B\rangle}\left(1 - \mathrm{erf}\left(\frac{|a|\sqrt{\pi}}{2\langle\Delta\tau_B\rangle}\right)\right), \quad a \in R. \tag{10}$$

Clearly, the same result holds also for Ω_{B2} and Ω_{B3}.

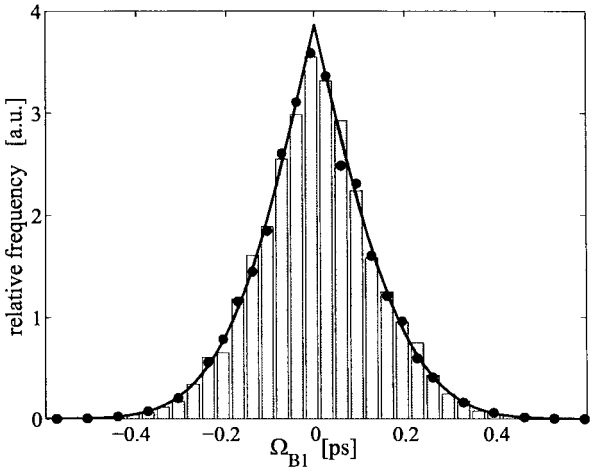

Fig. 1. PDF of Ω_{B1}: experimental results (vertical bars) and numerical results (black dots) are from [3] continuous line is the theoretical result (10).

Fig. 1 shows the experimental data (vertical bars) and the numerical results (black dots) published in [3]. Continuous line is the analytical pdf of Ω_{B1} as in (10), where $\langle \Delta\tau_B \rangle$ was set to the measured value of 0.2 ps. The agreement between theoretical, numerical and experimental results is fairly good.

III. Calculus of the Detected Power

As anticipated in the introduction, the backreflection fixed-polarizer method is based on the analysis of the power transmitted through a polarizer as a function of frequency, that can be expressed as follows:

$$T_B(\omega) = \frac{1}{2}(1 + \hat{s}_B(\omega) \cdot \hat{p}) \tag{11}$$

$\hat{p}$ being the Stokes vector representing the linear polarizer. Since the fiber is assumed with no losses, and since we are dealing with normalized power, also T_B is normalized between 0 and 1. By means of (2), (11) can be so rearranged

$$T_B = \frac{1}{2}(1 + (\mathbf{RM}\hat{p}) \cdot (\mathbf{MR}\hat{s}_0)) \tag{12}$$

and assuming the input field to be linearly polarized, and the output polarizer to be perfectly aligned to it ($\hat{p} = \hat{s}_0$), the detected power may be simplified as follows (please note that since $\hat{p}$ and $\hat{s}_0$ represent a linear SOP, their third component is zero)

$$T_B = \frac{1}{2}(1 + \hat{s}_F \cdot (\mathbf{M}\hat{s}_F)). \tag{13}$$

Finally, introducing (5) into (13), we obtain

$$T_B = \frac{1}{2}(1 + \cos 2\xi) = \cos^2 \xi. \tag{14}$$

Obviously, when the fiber is in the long length regime, $T_B(\omega)$ is a random quantity. With the help of (A5), it is easy to find its statistical description; in particular its cumulative distribution function (CDF) reads as[1]

$$\begin{aligned} F_{T_B}(\upsilon) &= \mathcal{P}[T_B \le \upsilon] = \mathcal{P}[\cos 2\xi \le 2\upsilon - 1] \\ &= 1 - \sqrt{1-\upsilon}, \quad \upsilon \in [0,1] \end{aligned} \tag{15}$$

where $\mathcal{P}[A]$ is the probability of the event A. The pdf can be calculated by taking the derivative of $F_{T_B}(\upsilon)$, which yields

$$f_{T_B}(\upsilon) = \frac{1}{2\sqrt{1-\upsilon}}, \quad \upsilon \in [0,1] \tag{16}$$

finally, the mean value of T_B results to be $2/3$.

Let us now find an explicit expression for the derivative of T_B with respect to ω. From (11) we have that $T_B' = (\hat{s}_B' \cdot \hat{p})/2$; using (3) and with the help of properties of orthogonal matrices [1], it results

$$\begin{aligned} T_B' &= \frac{1}{2}\bar{\Omega}_B \times \hat{s}_B \cdot \hat{p} = -\mathbf{MR}^T(\bar{\Omega}_L \times (\mathbf{MR}\hat{s}_0)) \cdot \hat{p} \\ &= -(\mathbf{RM}\hat{p}) \cdot (\bar{\Omega}_L \times (\mathbf{MR}\hat{s}_0)) \\ &= -\bar{\Omega}_L \cdot ((\mathbf{MR}\hat{s}_0) \times (\mathbf{RM}\hat{p})). \end{aligned}$$

Recalling that $\hat{p} = \hat{s}_0$, and that $\hat{p}$ represents a linear polarization, T_B' may be further simplified, leading to

$$T_B' = -\bar{\Omega}_L \cdot (\mathbf{M}\hat{s}_F) \times \hat{s}_F = -(\bar{\Omega}_L \cdot \hat{u}) \sin 2\xi \tag{17}$$

where $\hat{u} = (\sin\psi, -\cos\psi, 0)$.

IV. Analysis of Level Crossing Rate

We would like to investigate the relationship between the mean DGD and the mean value of the ratio $N_B(\upsilon)/\Delta\omega$, where $N_B(\upsilon)$ is the number of times $T_B(\omega)$ crosses the level υ in the frequency window $\Delta\omega$. This mean value can be found by means of the following formula [10]:

$$n_B(\upsilon) = E\left[\frac{N_B(\upsilon)}{\Delta\omega}\right] = f_{T_B}(\upsilon) E[|T_B'| : T_B = \upsilon] \tag{18}$$

where $E[x : y]$ is the expected value of x, given y. Let us notice that when $T_B = \upsilon$, then $\cos 2\xi = 2\upsilon - 1$. Consequently, (18) rearranges to:

$$n_B(\upsilon) = f_{T_B}(\upsilon) E[|\sin 2\xi||\bar{\Omega}_L \cdot \hat{u}| : \cos 2\xi = 2\upsilon - 1]$$

which further simplifies to

$$n_B(\upsilon) = 2 f_{T_B}(\upsilon)\sqrt{\upsilon(1-\upsilon)} E[|\bar{\Omega}_L \cdot \hat{u}| : \cos 2\xi = 2\upsilon - 1].$$

Now, let us assume that $\hat{s}_F(\omega)$ is statistically independent of $\bar{\Omega}_L(\omega)$ [8]. By means of (16), writing $\bar{\Omega}_L$ as in (8), $n(\upsilon)$ can be rewritten as follows:

$$n_B(\upsilon) = E[|\bar{\Omega}_L \cdot \hat{u}|]\sqrt{\upsilon} = \frac{1}{2}E[\Delta\tau_B]E[|\sin(\psi - \theta)|]\sqrt{\upsilon}.$$

Since $\psi \in \mathcal{U}(0, 2\pi)$, $E[|\sin(\psi - \theta)|] = E[|\sin\psi|] = 2/\pi$ (see Appendix C), and using (6), we finally find

$$\langle \Delta\tau \rangle = \frac{2 n_B(\upsilon)}{\sqrt{\upsilon}}. \tag{19}$$

[1] In this work we will give the statistical description of a random variable by means of either its pdf or its cumulative distribution function, together with the validity domain of the given expressions. Outside this domain, the functions are assumed to be zero or one, accordingly.

In particular, if we choose $v = 2/3$ (the mean level), then it results

$$\langle \Delta\tau \rangle = n_{m,B}\sqrt{6} \tag{20}$$

where $n_{m,B} = n_B(2/3)$. For comparison, we report the formula found in [8] for the "forward configuration"

$$\langle \Delta\tau \rangle = 4n_{m,F}. \tag{21}$$

V. Analysis of the Extrema

Counting the extrema of a signal is equivalent to counting the times its derivative crosses the zero level. Because of this the mean number of extrema of T_B over an unitary frequency band can be expressed as [10]

$$n_{e,B} = f_{T'_B}(0)E[|T''_B| : T'_B = 0]. \tag{22}$$

An analogous expression holds for the forward configuration, and in [8] it is shown that only the first factor can be theoretically calculated. On the contrary, when one is dealing with the backreflected signal, not even $f_{T'_B}(0)$ can be theoretically found, since the nonuniformity of T_B distribution complicates the equations. So we could investigate the relationship between $n_{e,B}$ and $\langle \Delta\tau \rangle$ only by a numerical analysis.

We described the fiber by means of the waveplate model described in Appendix D. Fibers were assumed to be made of 10 000 waveplates, while the ratio L_R/L_B ranged between 1 and 20 (L_R is the plate length and L_B is the mean beat-length of each waveplate). The signal $T_B(\omega)$ was simulated over 1000 nm, scanned in steps of 0.1 nm, at a center wavelength of 1500 nm. For each fiber the number of extrema was counted, not only of T_B, but also of the forward propagating fields. Results were averaged over an ensemble of 25 000 fiber.

Independently of the value assumed by L_R/L_B, we found the following relationship for the backreflected signal:

$$\langle \Delta\tau \rangle \simeq 1.555 n_{e,B}. \tag{23}$$

A similar equation holds for the extrema density in the forward configuration, and it reads

$$\langle \Delta\tau \rangle \simeq 2.534 n_{e,F} \tag{24}$$

the slight difference (2%) between [8, eq. (32)] and (24) is due to the different model adopted (see Appendix D). A similar comment has been already reported in [11].

VI. Source Bandwidth Influence

Theoretical results reported in Section IV require the knowledge of $T_B(\omega)$ for all the frequencies, which is practically impossible. Moreover, also numerical results of Section V were obtained using a band wider than those practically accessible. Because of this it is interesting to investigate the effects of a bounded bandwidth source.

Like in [8], we have numerically analyzed the following quantity:

$$\sigma^2 = \langle (\langle \Delta\tau \rangle_c - \langle \Delta\tau \rangle)^2 \rangle_{\text{fiber}} \tag{25}$$

where $\langle \Delta\tau \rangle$ is the theoretical mean DGD calculated by means of (D10), $\langle \Delta\tau \rangle_c$ is the value obtained from a single measure of $T_B(\omega)$ (using either extrema or crossing-level counting), and the symbol $\langle \cdot \rangle_{\text{fiber}}$ denotes an average carried out over an ensemble of 25 000 fibers.

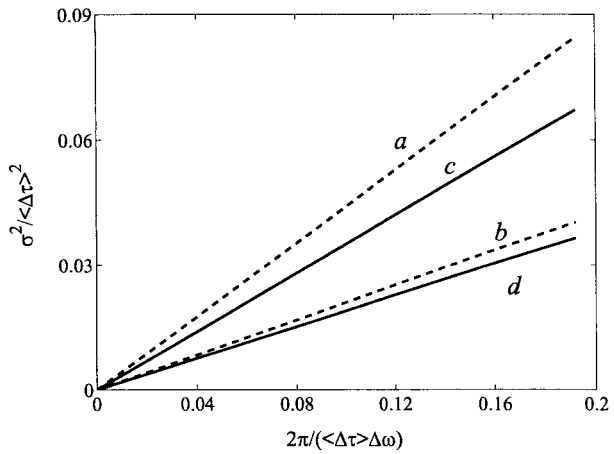

Fig. 2. Normalized DGD variance plotted as a function of the reciprocal bandwidth. Lines a, b, c, and d refer, respectively, to (26), (27), (28), and (29).

In forward configuration the following empirical relationships hold (even if the adopted numerical model is slightly different, these results are the same as those reported in [8])

$$\left.\frac{\sigma^2}{\langle \Delta\tau \rangle^2}\right|_{\substack{\text{forward}\\ \text{meanlevel}}} \simeq 0.44\frac{2\pi}{\langle \Delta\tau \rangle \Delta\omega} \tag{26}$$

$$\left.\frac{\sigma^2}{\langle \Delta\tau \rangle^2}\right|_{\substack{\text{forward}\\ \text{extrema}}} \simeq 0.21\frac{2\pi}{\langle \Delta\tau \rangle \Delta\omega} \tag{27}$$

where $\Delta\omega$ is the bandwidth. Similar expressions have been found also for the round-trip configuration, and they read

$$\left.\frac{\sigma^2}{\langle \Delta\tau \rangle^2}\right|_{\substack{\text{round trip}\\ \text{meanlevel}}} \simeq 0.35\frac{2\pi}{\langle \Delta\tau \rangle \Delta\omega} \tag{28}$$

$$\left.\frac{\sigma^2}{\langle \Delta\tau \rangle^2}\right|_{\substack{\text{round trip}\\ \text{extrema}}} \simeq 0.19\frac{2\pi}{\langle \Delta\tau \rangle \Delta\omega}. \tag{29}$$

As it was predictable, the relative error decreases as the bandwidth increases. It can also be noticed that measurements taken on the backreflected signal have a smaller uncertainty compared to the analogous taken in the forward configuration. This is clearly shown in Fig. 2, where lines a, b, c, and d refer, respectively, to (26), (27), (28), and (29).

VII. Analysis of the Spectral Density

Also the pseudointerferometric method can be modified to operate on the backreflected field. Following the guidelines traced out in [12], we can define a mean-shifted signal $P(\omega) = T_B(\omega) - 2/3$, and its correlation function $r_P(u) = E[P(\omega)P(\omega + u)]$. The Fourier transform of $r_P(u)$ is the spectral density of $P(\omega)$, $W_P(f)$, which reads as follows:

$$W_P(f) = \mathcal{F}[r_P(u)](f) = \int_R r_P(u)e^{-j2\pi fu}\,du.$$

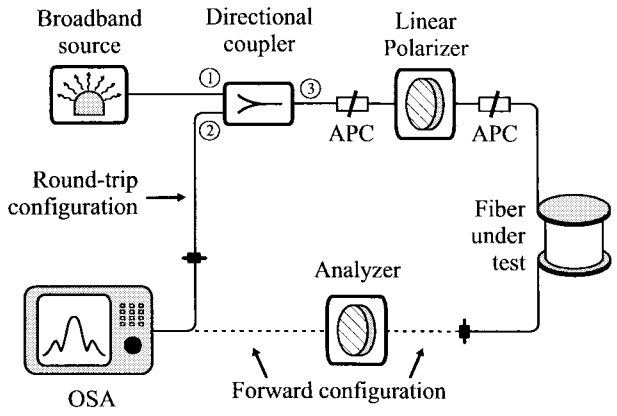

Fig. 3. Schematic experimental setup.

Because $r_P(u)$ is an even real function, the same holds for $W_P(f)$, which has a zero mean and whose variance reads

$$\sigma^2_{W,B} = \frac{\int_R f^2 W_P(f)\, df}{\int_R W_P(f)\, df}. \tag{30}$$

Using the rules of Fourier calculus, we can rearrange expression (30) (with respect to [12], the factor $1/4\pi^2$ is due to a different definition of the Fourier transform):

$$\sigma^2_{W,B} = -\frac{1}{4\pi^2}\frac{r''_P(0)}{r_P(0)}$$

moreover, since $r''_P(u) = -E[P'(\omega)P'(\omega+u)$ [10], we find

$$\sigma^2_{W,B} = \frac{E[(P')^2]}{4\pi^2 E[P^2]} \tag{31}$$

and using (14) and (17) it results (see also Appendix C)

$$\sigma^2_{W,B} = \frac{E[\Delta\tau_B^2]E[\sin^2(\psi-\theta)]E[\sin^2 2\xi]}{16\pi^2 E\left[\left(\cos^2\xi - \frac{2}{3}\right)^2\right]} = \frac{3E[\Delta\tau_B^2]}{16\pi^2}.$$

Finally, recalling that $\Delta\tau_B$ is Rayleigh distributed and hence $E[\Delta\tau_B^2] = (4/\pi)E[\Delta\tau_B]^2 = \pi E[\Delta\tau]^2$, the searched relationship reads

$$\langle\Delta\tau\rangle = 4\sqrt{\frac{\pi}{3}}\sigma_{W,B}. \tag{32}$$

As before, let us report the analogous result for the "forward configuration" (which can be derived from [12])

$$\langle\Delta\tau\rangle = 4\sqrt{\pi}\,\sigma_{W,F}. \tag{33}$$

VIII. Experiment

The previous theoretical relationships have been verified by the experimental setup shown in Fig. 3. The optical source, a broad-band super-luminescent LED (with a 100 nm bandwidth, centered at 1550 nm), is connected to port 1 of a polarization-insensitive directional coupler. The optical radiation is then passed through a bidirectional, all-fiber, linear polarizer, and finally injected into the fiber under test. Please note that connections between the coupler and the polarizer, and between the latter and the fiber should be done by means of an angled connector (FC/APC), in order to reduce as much as possible all those backreflections which could overlap the far-end contribution. The optical spectrum analyzer (OSA) is connected to port 2 of the coupler to collect backreflection or, alternatively, to the fiber far-end, in a classical forward configuration, as described in [8].

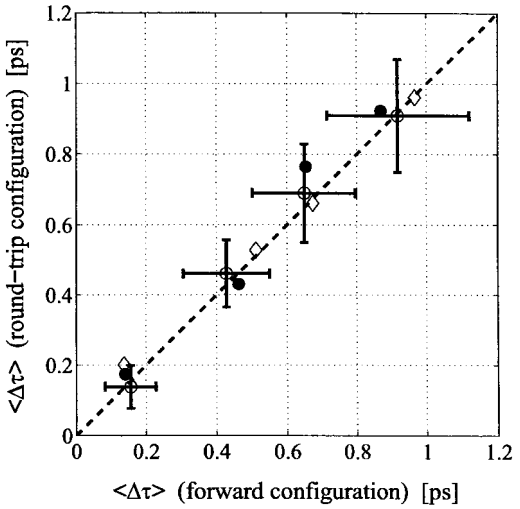

Fig. 4. Values of $\langle\Delta\tau\rangle$ measured in the round-trip configuration versus $\langle\Delta\tau\rangle$ measured in the forward configuration. Filled dots refer to the PI analysis, empty circles to the crossing counting, and empty diamonds to the extrema counting. Error bars refer to the level crossing analysis.

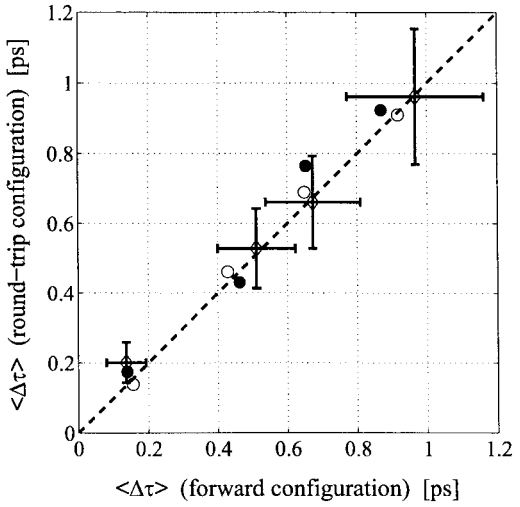

Fig. 5. Values of $\langle\Delta\tau\rangle$ measured in the round-trip configuration versus $\langle\Delta\tau\rangle$ measured in the forward configuration. Filled dots refer to the PI analysis, empty circles to the crossing counting, and empty diamonds to the extrema counting. Error bars refer to the extrema density analysis.

Measurements were performed over a set of 4 single-mode, step-index fibers with length ranging from 3 km up to 20 km. For each link, the spectrum of the backreflected and of the transmitted power, without any polarizing element was measured and stored. These data were subsequently used to normalize the signals between 0 and 1. Fifteen spectra were measured for each fiber length, both in the forward and round-trip configuration, with a delay of at least 2 hours between each measurement.

Experimental results are reported in Figs. 4 and 5. In both figures the horizontal axis reports the mean DGD measured

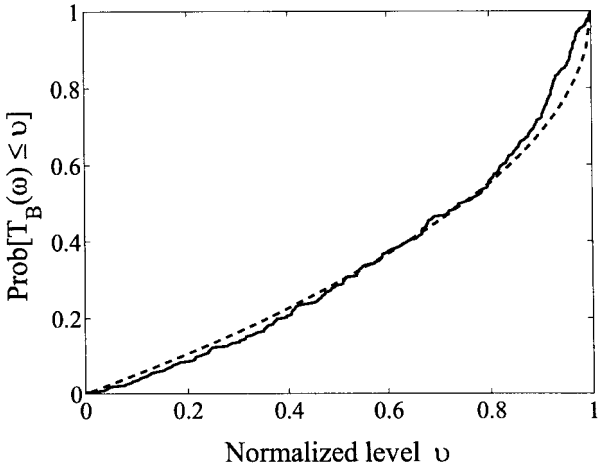

Fig. 6. CDF of $T_B(\omega)$: the continuous line refers to experimental data, while the dashed line is the theoretical result (15).

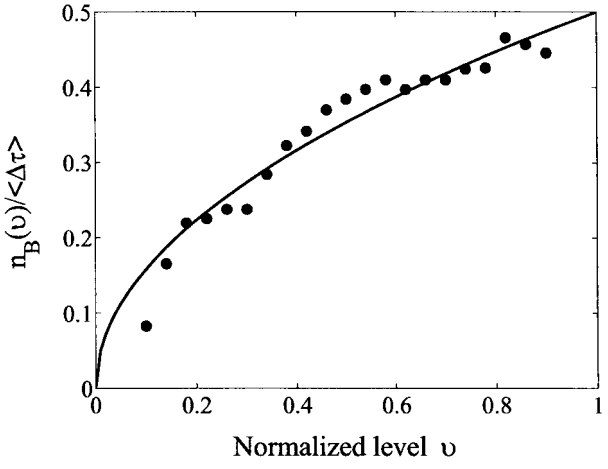

Fig. 7. Evolution of the normalized level crossing rate as a function of level. The continuous line is the theoretical result (19), while the filled dots represent the experimental data.

in the forward configuration, while the vertical axis reports the value measured in the round-trip configuration. Circles refers to measurements performed by means of the mean-level crossing counting [i.e., (20) and (21)], diamonds are measures made by extrema counting [(23) and (24)] and filled dots refers to value obtained by means of the pseudointerferometric method [(32) and (33)]. The power spectral density was estimated by means of the following formula [13]:

$$W_P(f) \simeq \frac{1}{\Delta\omega}\left(\frac{1}{N}\sum_{n=1}^{N}|\mathcal{F}[P_n](f)|^2\right)$$

where N is the number of the measured evolution of $P(\omega)$, and $\Delta\omega$ is the source bandwidth. In Fig. 4 horizontal and vertical bars represent respectively the uncertainty of the level crossing analysis in forward and in round-trip configuration, according to what reported in Section VI. In the same way, bars reported in Fig. 5 represent the uncertainty of the extrema counting technique. A good agreement is evident between the three measurement methods, both in forward and round-trip configuration.

The same experimental data had been differently elaborated to produce Figs. 6 and 7. The former illustrates the comparison between the theoretical CDF of $T_B(\omega)$ [(15), dashed line in the figure] with the experimental one (continuous line). The latter reports $n_B(\upsilon)/\langle\Delta\tau\rangle$ as a function of the level υ, both theoretically [continuous line in the figure, obtained rearranging (19)], and experimentally (black dots). Both figures show a good correspondence between theory and experiment.

IX. Conclusion

We derived analytical expressions and numerical relationships for single-end PMD measurements based on the fixed-polarizer method. In particular we related the mean value of the DGD to arbitrary-level crossing density, extrema density and standard deviation of the backreflected power spectral density. Analytical, numerical and experimental results are in very good agreement. We estimated also the effect of the limited bandwidth on the measurement accuracy. Finally, we analytically found the pdf of the polarization dispersion vector of the round-trip.

Appendix A
Statistical Description of $\hat{s}_F$

When a polarized signal propagates through a lossless, randomly birefringent fiber in the long length regime, its state of polarization, $\hat{s}_F$, is a random unit vector that uniformly covers the Poincaré sphere [8].

Let $\hat{s}_F$ be expressed as in (5). In order to find the statistical description of the angular coordinates ψ and ξ, we calculate the probability of the event $\{\hat{s}_F \in \mathcal{A}\}$, where $\mathcal{A}$ is an infinitesimal area, centered around a point of azimuth $\theta \in [0, 2\pi]$ and zenith $\phi \in [-\pi/2, \pi/2]$. We can write

$$\mathcal{P}[\hat{s}_F \in \mathcal{A}] = f_{\psi,\xi}(\theta,\phi)\,d\theta\,d\phi \tag{A1}$$

with $f_{\psi,\xi}(\theta,\phi)$ the joint probability density function of ψ and ξ evaluated in (θ,ϕ). On the other hand, $\hat{s}_F$ is uniformly distributed on the sphere, so it also results

$$\mathcal{P}[\hat{s}_F \in \mathcal{A}] = \frac{\mathrm{meas}(\mathcal{A})}{4\pi r^2} \tag{A2}$$

where r is the radius of the sphere, and $\mathrm{meas}(\mathcal{A}) = r^2\cos\phi\,d\phi\,d\theta$ is the measure of $\mathcal{A}$. By equating (A1) with (A2), we can now state that

$$f_{\psi,\xi}(\theta,\phi) = \frac{1}{4\pi}\cos\phi.$$

The evaluation of the marginal densities leads to the following pdf's [10]:

$$\psi \in \mathcal{U}(0,2\pi) \quad \text{hence } f_\psi(\theta) = \frac{1}{2\pi} \tag{A3}$$

$$f_\xi(\phi) = \frac{1}{2}\cos\phi, \quad \phi \in \left[-\frac{\pi}{2}, \frac{\pi}{2}\right]. \tag{A4}$$

Using these results and developing cumbersome calculations not reported for the sake of brevity, it is possible to show that the three components of the vector $\hat{s}_F$ are uniformly distributed between -1 and 1. Moreover, $f_\psi(\theta)f_\xi(\phi) =$

$f_{\psi,\xi}(\theta,\phi)$ and this demonstrates that ψ and ξ are statistically independent.

Using (A4) we can find the statistical description of $x = \cos 2\xi$, that is

$$\begin{aligned} F_x(a) &= \mathcal{P}[\cos 2\xi \le a] \\ &= \mathcal{P}\left[\xi \ge \frac{1}{2}\arccos a\right] + \mathcal{P}\left[\xi \le -\frac{1}{2}\arccos a\right] \\ &= 1 - F_\xi\left(\frac{1}{2}\arccos a\right) + F_\xi\left(-\frac{1}{2}\arccos a\right) \\ &= 1 - \sin\left(\frac{1}{2}\arccos a\right) \end{aligned}$$

which by means of trigonometric formulae leads to

$$F_x(a) = 1 - \sqrt{\frac{1-a}{2}}, \quad a \in [-1,1]. \tag{A5}$$

Appedix B
Calculation of (10)

Let it be $w = xy$, where $x \in \mathcal{U}(-1,1)$, and y is Rayleigh distributed, so that its pdf reads as

$$f_y(b) = \frac{\pi b}{2m^2}\exp\left(-\frac{\pi b^2}{4m^2}\right)$$

$m = E[y]$ being the mean value of y. Moreover, let us assume that the two variables are statistically independent.

The cumulative distribution function (CDF) of w can be calculated by means of the total probability theorem, which yields

$$F_w(a) = \int_0^{+\infty} \mathcal{P}[xy \le a : y = b] f_y(b)\, db$$

where $\mathcal{P}[A \mid B]$ is the probability of the event A, given B. Since the pdf of w is an even function, we limit the analysis to the case $a \ge 0$; moreover, the CDF of x reads

$$F_x(c) = \begin{cases} 1, & \text{if } c > 1 \\ (1+c)/2, & \text{if } 0 \le c \le 1 \\ 0, & \text{if } c < 0, \end{cases}$$

so that we have

$$\begin{aligned} F_w(a) &= \int_0^{+\infty} \mathcal{P}\left[x \le \frac{a}{b}\right] f_y(b)\, db \\ &= \int_0^a f_y(b)\, db + \int_a^{+\infty} \frac{a+b}{2b} f_y(b)\, db. \end{aligned}$$

By taking the derivative with respect to a, we find the pdf of w

$$f_w(a) = \int_a^{+\infty} \frac{\pi}{4m^2}\exp\left(-\frac{b^2}{\pi m^2}\right) db$$

integrating and extending the result also to negative values, we finally find

$$f_w(a) = \frac{\pi}{4m}\left(1 - \operatorname{erf}\left(\frac{|a|\sqrt{\pi}}{2m}\right)\right), \quad a \in R. \tag{B6}$$

Appendix C
A Useful Result

The results to be presented in this section may be found also in [14]. We report them here for completeness.

Let θ be uniformly distributed between 0 and 2π, and let α be a random variable, statistically independent of θ, whose pdf may be unknown. The characteristic function of the random variable $x = \sin(k\theta+\alpha)$ (k any integer but not zero) reads [10]

$$\Psi_x(u) = E\left[e^{ju\sin(k\theta+\alpha)}\right] = E\left[E\left[e^{ju\sin(k\theta+\alpha)} : \alpha\right]\right]. \tag{C7}$$

Because of the statistical independence between θ and α, the innermost expected value of last expression may be evaluated as if α was a constant value, so that it results

$$\begin{aligned} E\left[e^{ju\sin(k\theta+\alpha)} : \alpha\right] &= E\left[e^{ju\sin(k\theta+\alpha)}\right] \\ &= \frac{1}{2\pi}\int_0^{2\pi} e^{ju\sin(k\theta+\alpha)}\, d\theta. \end{aligned} \tag{C8}$$

Let us define $\mu = k\theta + \alpha$; using the periodicity of the sine function the last integral may be rearranged as

$$\frac{1}{2\pi}\int_0^{2k\pi} \frac{1}{k} e^{ju\sin\mu}\, d\mu = \frac{1}{2\pi}\int_0^{2\pi} e^{ju\sin\mu}\, d\mu = J_0(u)$$

where $J_0(u)$ is the Bessel function of the first kind of zero order [15]. It should be noted that this result does not depend anymore on α, so it is easy to evaluate the outermost expected value of (C7), which finally yields

$$\Psi_x(u) = E[J_0(u)] = J_0(u).$$

Consequently, statistical properties of x depend only on θ.

The pdf of x is the inverse Fourier transform of $\Psi_x(-u)$ [10], so that it results

$$\begin{aligned} f_x(a) &= \frac{1}{2\pi}\int_{-\infty}^{+\infty} J_0(u) e^{-jua}\, du \\ &= \frac{1}{\pi}\int_0^{+\infty} J_0(u)\cos(ua)\, du \end{aligned}$$

and, hence, we find [15]

$$f_x(a) = \frac{1}{\pi\sqrt{1-a^2}}, \quad x \in [-1,1]. \tag{C9}$$

Appendix D
Numerical Model of a Fiber

Fibers can be numerically studied by means of the well known waveplate model. Differences may occur in the implementation of this model, due to the statistical properties of the waveplates. In [8] all waveplates were supposed to have the same DGD; however with this choice the signal T_B is periodic as noted in [11].

Because of this, we assume that the waveplates are statistically independent of each other, both in terms of beat-length and birefringence axes rotation. In fact, let $\vec{\beta} = (\beta_1, \beta_2, 0)$ be the local birefringence vector, then we assume that β_1 and β_2 are statistically independent Gaussian random variables, with zero mean and the same standard deviation. The waveplate optical axes are uniformly distributed between 0 and 2π,

while the modulus of the birefringence, $b = |\bar{\beta}|$, is Rayleigh distributed [16].

The DGD of each plate is [8]

$$d\tau = \frac{\lambda b}{2\pi c} L_R$$

where L_R is the waveplate length (assumed constant); clearly, $d\tau$ is Rayleigh distributed. The total mean DGD of the fiber can be calculated from [8] as follows:

$$\langle \Delta\tau^2 \rangle = \sum_{i=1}^{N} \langle d\tau_i^2 \rangle = N \langle d\tau^2 \rangle = \frac{4N}{\pi} \langle d\tau \rangle^2$$

where N is the number of waveplates. When a fiber is in the long-length regime, $\Delta\tau$ is Maxwellian. If we define the beat-length as $L_B = 2\pi/\langle b \rangle$, we finally obtain

$$\langle \Delta\tau \rangle = \sqrt{\frac{4}{\pi}} \sqrt{\frac{8N}{3\pi}} \langle d\tau \rangle = \frac{4}{\pi} \sqrt{\frac{2N}{3}} \frac{\lambda L_R}{c L_B}. \tag{D10}$$

REFERENCES

[1] F. Corsi, A. Galtarossa, and L. Palmieri, "Polarization mode dispersion characterization of single-mode optical fiber using backscattering technique," *J. Lightwave Tech.*, vol. 16, pp. 1832–1843, Oct. 1998.

[2] F. Corsi, A. Galtarossa, and L. Palmieri, "Beat-length measurment in highly mode-coupled single-mode fibers by means of Fourier transform of backscattered signal," in *Proc. Tech. Dig. Symp. Optic. Fiber Measurement*, Boulder, CO, 1998, pp. 105–108.

[3] F. Corsi, A. Galtarossa, L. Palmieri, M. Schiano, and T. Tambosso, "Continous-wave back-reflection measurement of polarization mode dispersion," *IEEE Photon. Technol. Lett.*, vol. 11, pp. 451–453, Apr. 1999.

[4] F. Corsi, A. Galtarossa, and L. Palmieri, "Analytical treatment of polarization dispersion in single-mode fibers by means of backscattering signal," *J. Opt. Soc. Amer. A*, vol. 16, pp. 574–583, Mar. 1999.

[5] E. Brinkmeyer, "Forward-backward transmission in birefringent single-mode fibers: Interpretation of polarization-sensitive measurements," *Opt. Lett.*, vol. 11, pp. 575–577, 1981.

[6] Technical Staff of CSELT, *Fiber Optic Communications Handbook*, F. Tosco, Ed. Blue Ridge Summit, PA: TAB Books, 1990.

[7] C. D. Poole and J. Nagel, "Polarization effects in lightwave systems," in *Optical Fiber Telecommunications*, I. P. Kaminow and T. Koch, Eds. San Diego, CA: Academic, 1997.

[8] C. D. Poole and D. L. Favin, "Polarization-mode dispersion measurement based on transmission spectra through a polarizer," *J. Lightwave Technol.*, vol. 12, pp. 917–929, 1994.

[9] M. K. Simon, S. M. Hinedi, and W. C. Lindsey, *Digital Communication Techniques*. Englewood Cliffs, NJ: Prentice-Hall, , 1995.

[10] A. Papoulis, *Probability, Random Variables and Stochastic Processes*. New York: McGraw-Hill, 1984, pp. 345–353.

[11] P. A. Williams and C. M. Wang, "Corrections to fixed analyzer measurements of polarization mode dispersion," *J. Lightwave Technol.*, vol. 16, pp. 534–541, 1998.

[12] B. L. Heffner, "Influence of optical source characteristics on the measurement of polarization-mode dispersion of highly mode-coupled fibers," *Opt. Lett.*, vol. 21, pp. 113–115, 1996.

[13] S. M. Kay, *Modern Spectral Estimation—Theory & Application*. Englewood Cliff, NJ: Prentice-Hall, 1988.

[14] F. Corsi, A. Galtarossa, and L. Palmieri, "Beat-length characterization based on backscattering analysis in randomly perturbed single-mode fibers," *J. Lightwave Technol.*, vol. 17, pp. 1172–1178, July 1999.

[15] I. S. Gradshteyn and I. M. Ryzhik, *Table of Integrals, Series, and Products*, A. Jeffrey, Ed. San Diego, CA: Academic, 1994.

[16] P. K. A. Wai and C. R. Menyuk, "Polarization mode dispersion, decorrelation, and diffusion in optical fibers with randomly varying birefringence," *J. Lightwave Technol.*, vol. 14, pp. 148–157, 1996.

Andrea Galtarossa (M'88) received the degree in electronic engineering from the University of Padova, Italy, in 1984.

In 1986, he received a Postgraduate fellowship from Telettra Spa, Vimercate (IT), Italy, for research in WDM components. In 1987, he joined Saifo srl, Padova (IT), Italy, a private company involved in measurements and teaching in optical systems. In 1990, he became Assistant Professor in Electromagnetic Fields at DEI, University of Padova. In 1998, he became Associate Professor in Microwave at the same university. He is the author or coauthor of more than 60 papers. His current research activity is mainly in birefringent fibers and PMD measurements and modeling.

Luca Palmieri (M'95) was born in Belluno, Italy, in 1971. In 1996, he received the degree in electronic engineering from the University of Padova, Italy, He is currently working towards the Ph.D. degree at the same university.

Since 1998 he is also cooperating with CSELT (Torino) in the field of PMD measurement. His research activity is focused on PMD, and in particular, PMD measurement techniques and systems impairment due to PMD.

Marco Schiano (M'92) received the degree in electronic engineering from the University of Padova, Italy, in 1990.

Since then he has been involved in research activities in the field of fiber-optic measurements. In 1997, he joined the Transmission and Optical Technology Division of CSELT, Torino, Italy, where he is now working in the Optical Carriers Department. His current interests are the characterization of optical fibers and components and the development of high-speed transmission systems.

Tiziana Tambosso (M'94) received the M.S. and Ph.D. degrees in optoelectronic engineering from University of Pavia, Italy, in 1983 and 1988, respectively.

After a period spent with SGS—Thomson, working on design and development of bipolar electronic circuits for telecommunication applications, she has been a Researcher at University of Pavia working on fiber-optic passive components and fiber optic sensors. From 1989 to 1993, she has been responsible for the fiber-optic devices group at SIRTI, R&D Division, developing optical fiber couplers, attenuators and amplifiers. In 1993, she joined CSELT, the Telecom Italia Group R&D laboratories, where she has been working on second window fiber-optic amplifiers and since 1996 she has been the head of a group on passive optical components measurement, reliability and standardization. From 1993 to 1997, she has been the Secretary of IEC Subcommittee SC86B on fiber-optic interconnecting devices and passive components. She holds eight patents and has authored forty papers.

Dr. Tambosso is a member of AEI and IEEE and the Secretary of IEEE LEOS Italian Chapter.